

VeriBug: An Attention-based Framework for Bug-Localization in Hardware Designs

Giuseppe Stracquadanio^{1,2*}, Sourav Medya¹, Stefano Quer² and Debjit Pal¹

¹University of Illinois Chicago, Chicago, IL, USA ²Politecnico di Torino, Torino, Italy
{gstrac3, medya, dpal2}@uic.edu, stefano.quer@polito.it

Abstract—In recent years, there has been an exponential growth in the size and complexity of System-on-Chip designs targeting different specialized applications. The cost of an undetected bug in these systems is much higher than in traditional processor systems as it may imply the loss of property or life. The problem is further exacerbated by the ever-shrinking time-to-market and ever-increasing demand to churn out billions of devices. Despite decades of research in simulation and formal methods for debugging and verification, it is still one of the most time-consuming and resource intensive processes in contemporary hardware design cycle. In this work, we propose VeriBug, which leverages recent advances in deep learning to accelerate debugging at the Register-Transfer Level and generates explanations of likely root causes. First, VeriBug uses control-data flow graph of a hardware design and learns to execute design statements by analyzing the context of operands and their assignments. Then, it assigns an importance score to each operand in a design statement and uses that score for generating explanations for failures. Finally, VeriBug produces a heatmap highlighting potential buggy source code portions. Our experiments show that VeriBug can achieve an average bug localization coverage of 82.5% on open-source designs and different types of injected bugs.

I. INTRODUCTION

Simulation and formal verification are two complementary verification techniques. Given a design property, formal verification proves the property holds for every point of the search space. Simulation verifies the property by pseudo-randomly testing a small subset of the search space. The main drawback of the former is its unscalability, whereas the obvious flaw of the second is its inability to prove that a property holds for every point of the search space. With these limitations and the ever-increasing time-to-market and design complexity, developing new hardware and software verification methods is mandatory.

In this work, we specifically focus on bug localization in hardware designs. Bug localization techniques relying on formal methods, such as Binary Decision Diagrams (BDDs) [3], Bounded Model Checking (BMC) [4], Interpolants [7], IC3 [2], and other SAT-based methods offer a systematic and rigorous approach to identifying and localizing bugs in hardware designs. However, they are computationally intensive, require additional expertise, and imply conspicuous effort for specifying complex mathematical logic models. At the same time, bug localization in simulation-based workflows is addressed by collecting failure traces and identifying common patterns [9]. Patterns corresponding to common paths in failure runs can be mapped to the original source code to identify suspicious

code zones that require further inspection. A critical problem is that the localized suspicious code zones lack explanation and may provide not much information about the actual bug. Consequently, it is crucial to develop smarter techniques to reveal problems and localize them.

To reduce the gap between standard verification and everyday simulation techniques, we propose VeriBug, an automated bug-localization framework that harnesses the power of a data-driven approach and machine learning (ML). ML techniques for bug detection and localization have been studied in the software domain. However, we identify two main drawbacks of these approaches: (i) They directly extract features from specific code [11] and do not guarantee generalization to unseen code structures, and (ii) They approach the problem as a *classification* task, where an entire program is classified as buggy or not buggy [6], based on features extracted from a *static* analysis. These approaches suffer from poor generalization and require building a dataset with many programs containing one or more bugs. As such datasets are not readily available, this task becomes challenging.

These two limitations can also be transposed to the hardware domain. To overcome them, VeriBug does not rely on code characteristics, but automatically learns features from lower abstraction levels, such as Abstract Syntax Trees (ASTs). These learned features are *design-agnostic*, allowing VeriBug to generalize on unseen designs without any retraining. We learn execution semantics with a novel deep-learning architecture and use it to localize the root cause of a bug via comparison of learned semantics for failure and correct simulation traces. VeriBug does not need to be trained on a labeled design corpus as we train it on a *proxy*-task to learn execution semantics directly from simulation traces. Our approach is fully integratable with current verification workflows without requiring additional time or artifacts.

Our primary contributions are the followings: (i) VeriBug represents the first approach to bug localization in hardware designs that automatically learns task-relevant features in a inductive and generalizable setting, (ii) We learn execution semantics features using free supervision by simulation traces and we show how these features can be used for providing bug localization insights and producing a localization heatmap, (iii) We show learned knowledge is transferable and generalizable to unseen designs, and (iv) We conduct a bug injection campaign on 4 different real designs, obtaining an average coverage of 82.5% and localizing 85 injected bugs over a total of 103

*Work done while Giuseppe was studying toward his Master's degree. This work was funded by a startup fund from UIC.

observable bugs.

II. PRELIMINARIES

A Static Analyzer for Hardware Designs: GOLDMINE is an open-source hardware design analysis framework [8]. It takes the design source code as input and performs light-weight source code analysis. Moreover, GOLDMINE produces multiple artifacts, a few of which are: (i) Control-data flow graph (CDFG), which captures control flow and data flow among design variables, (ii) Variable dependency graph (VDG), which summarizes the control and data dependencies among design variables by abstracting operation details among design variables, and (iii) Cone-of-influence (COI) which captures the temporal relations among design variables when a design is unrolled for n cycles. In this work, we have extensively used GOLDMINE-generated CDFG, VDG, and testbenches for developing VeriBug.

Attention Networks: The attention mechanism has been originally developed to improve the performances of encoder-decoder systems for the machine translation tasks [1]. It weighs the relevance of each word in the input sequence when generating the next word of the output sequence. The attention mechanism generally allows neural networks to focus only on the important parts of the input data. We use dot-product attention to learn operand influence in design execution.

Recurrent Neural Networks: Recurrent Neural Networks (RNNs) [10] are a class of Artificial Neural Networks (ANN) tailored to process sequential data. RNNs maintain an *internal state* or *memory* of previous inputs. This inherent memory makes them particularly suitable for scenarios where past information influences decision-making. Besides being used to make predictions on sequential data, RNNs exhibit remarkable effectiveness in *embedding* variable-length sequential data into a compact, fixed-size embedding vector. In this work, we use a sophisticated RNN model, Long-Short Term Memory (LSTM), to generate representations of variable-length node paths in Abstract Syntax Trees (ASTs) of design source code.

III. BUG LOCALIZATION AS LEARNING PROBLEM

We aim to root-cause a design failure and localize it to a subset of the design source code. *Given a Verilog hardware design \mathbf{D} with \mathbf{I} inputs, \mathbf{O} outputs, and an observed failure f at output $t \in \mathbf{O}$, VeriBug localizes the failure to a subset of likely suspicious source code fragments $\mathcal{S} \in \mathbf{D}$ and generates quantitative explanations of suspiciousness as such.*

Workflow and insights: Figure 1 shows the complete workflow of VeriBug. Given a design \mathbf{D} , an input vector \mathbf{I}_n , a set of correct simulation traces \mathcal{T}_c , and set of failure simulation traces \mathcal{T}_f , we propose to learn Verilog execution semantics automatically and use the learned knowledge to assign *importance scores* to design statement operands. An insight is that these importance weights, computed using the concept of *attention*, contain critical design execution information that can be leveraged to *generate explanations for design failures*. After that, we aggregate such importance weights to concisely represent the design execution in passing failure traces. The aggregation

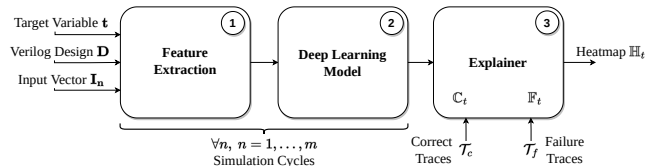


Fig. 1: **VeriBug workflow.** (1) The Feature Extraction component extracts *features* from the dynamic analysis of the design. (2) The Deep-Learning Model learns execution semantics using these features to predict target values. (3) The Explainer component aggregates trace-level semantics into condensed execution information, producing final heatmap \mathbb{H}_t .

results in two different maps, \mathbb{F}_t and \mathbb{C}_t , respectively, for failing and correct traces. Then, we compute a *suspiciousness score* for each design statement $l_k \in \mathbf{D}$ as $\mathbf{d}(\mathbb{F}_t(l_k), \mathbb{C}_t(l_k))$, where \mathbf{d} is a normalized norm-1 distance and $\mathbb{F}_t(\cdot)$ ($\mathbb{C}_t(\cdot)$) are the aggregated importance scores for a statement l_k in the aggregated map \mathbb{F}_t (\mathbb{C}_t). When the *suspiciousness score* for l_k is higher than a threshold, we store $\mathbb{F}_t(l_k)$ importance scores in a final heatmap \mathbb{H}_t . Eventually, these score can be mapped back to RTL code to provide further visual guidance in locating the root cause.

IV. PROPOSED METHODOLOGY: VERIBUG

A. Overview of VeriBug architecture

VeriBug introduces a novel bug-localization technique powered by a *deep learning* (DL) architecture. Its architecture consists of three key components: (i) Feature extraction, (ii) Deep learning model, and (iii) Explanation generation. We have summarized our proposed framework in Figure 1.

B. Feature extraction

The first component *Feature extraction* extracts knowledge (*i.e.*, features) from the input design \mathbf{D} . Figure 2 presents an illustration of this entire module consisting three steps. We use GOLDMINE to extract a Control Data Flow Graph (CDFG) and a Variable Dependency Graph (VDG) of the Verilog design \mathbf{D} , and to generate a *testbench* to simulate the design.

Dependence analysis: We perform a *dependence analysis* on the VDG to identify the set Dep_t of the *control* and *data* dependencies for t , as shown in Figure 2(1). This set is computed by reversing edges in the VDG and by starting a *Depth First Search* (DFS) from the target node t . All the nodes that can be visited through a DFS are added to Dep_t .

Design slicing: We use target variable t on the CDFG to extract design slices. Our slicing criterion simply includes a statement in the slice if the left-hand side (LHS) variable is in Dep_t . The slicing criterion is directly applied on complete CDFG of a design. Furthermore, we exclude program slices involving branches which cannot be executed by a given input vector \mathbf{I}_n . Intuitively, if a statement is not *executed* by \mathbf{I}_n , then it is certainly not the cause of a bug symptomatized at one of the outputs. After extracting all relevant statements, we translate them into Abstract Syntax Trees (ASTs) for further analysis. In Figure 2(1), we chose `gnt1` as t and use DFS to find $\text{Dep}_t = \{\text{req1}, \text{req2}, \text{state}\}$. We use `gnt1` and

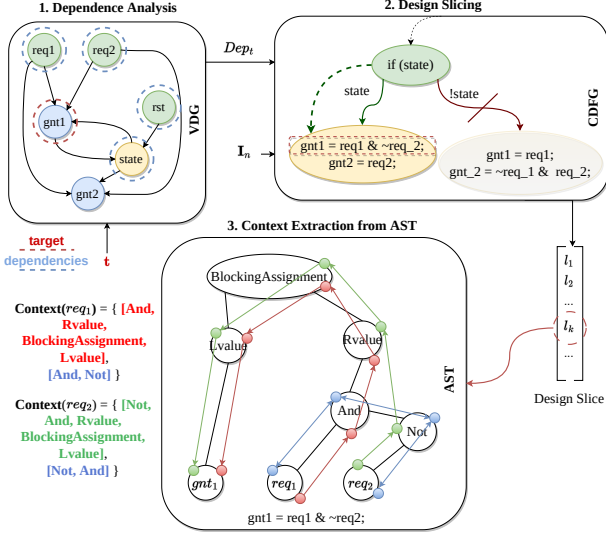


Fig. 2: **Feature Extraction Module.** (1) A dependence analysis produces the complete set Dep_t of control and data dependencies for the target output variable t . (2) The slicing criterion uses the extracted set of dependencies Dep_t and the input vector \mathbf{I}_n (e.g. $\{req1 = 0, req2 = 1, \dots\}$) to dynamically slice the input design \mathbf{D} . (3) Context extraction is finally achieved for the operands of each slice statement, after encoding them to Abstract Syntax Trees (ASTs) In the figure, the context of req_1 is the list of paths $\{[And, Rvalue, BlockingAssignment, Lvalue], [And, Not]\}$. an input $\mathbf{I}_n = \{req1 = 0, req2 = 1, \dots\}$ to extract the dynamic slice comprising the green and the yellow ellipses in Figure 2(2). Figure 2(3) shows the AST of one of the design statements $gnt1 = req1 \& \sim req2$ in the dynamic slice.

Context extraction from ASTs: The root node of an AST is the assignment type and the leaves are the input operands and the output variable. For the sake of brevity, we indicate the set of leaf nodes for the AST of l_k as $\mathcal{L}(l_k)$. In Figure 2(3), the root node is of *BlockingAssignment* type whereas the leaf nodes are variables, e.g., $req1$, $req2$, etc. We encode the relative structural information within an AST using *leaf-to-leaf* paths. We extract all the paths for each input operand op_i from the AST, i.e., $op_i \rightarrow op_k, \forall op_k \in \mathcal{L}(l_k) \setminus \{op_i\}$. In Figure 2(3), $req1 \rightarrow And \rightarrow Not \rightarrow req2$ is one such path. As this list represents the structural information for each operand, we refer it as the *context of the operand* in a statement.

C. Our Deep-learning model

The deep learning model leverages extracted knowledge from the feature extractor to learn *RTL execution semantics*. Figure 3 shows an overview of our model. We formulate the learning problem as – *predicting the output values of each executed statement using a combination of the input assignments and the context features as the input to our model*. This formulation allows us to use signal values from the simulation traces as training data for supervision without requiring any labels.

Our learning task: For each statement l_k sampled from the training set, the model aims to predict the output value assigned to the LHS of l_k , given input assignments in \mathbf{I}_n . VeriBug

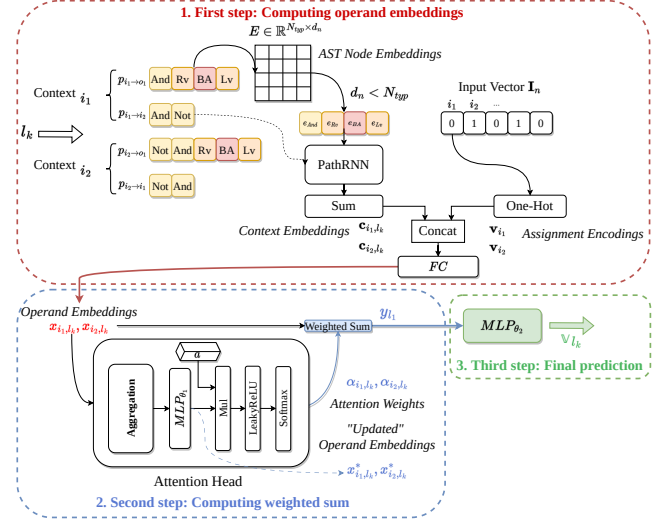


Fig. 3: **The Deep Learning Model of VeriBug.** (1) For each statement l_k and its AST, the model embeds operand contexts and encode their assignments to concatenate them in operand embeddings. (2) A weighted sum is computed with operand embeddings, using attention weights produced by our attention module. (3) A final prediction for l_k output value is made from a statement-level embedding produced by weighted sum.

learns to execute statements using operands’ *contexts* and their *assignments*. To predict output values, VeriBug assigns an attention weight (i.e., an importance score) to each operand in a statement. We use these attention weights for *debugging* and *bug localization* as they reveal *explanation* about the execution.

Operand embeddings: As mentioned above, VeriBug learns to execute statements using the information about the operands. Thus, our model VeriBug first generates expressive representations for each operand by embedding the contexts of operands from the AST and the assignments in two fixed-sized vectors. Specifically, for each path in a context (see an example of a context with multiple paths in Fig. 2), a LSTM model, referred as *PathRNN* at Figure 3, is employed to produce a *path embedding* $\mathbf{p}_{i \rightarrow j} \in \mathbb{R}^{d_c}$ from the paths consisting of sequence of nodes in the AST, where i denotes the operand node and j denotes other leaf nodes. As there are several paths in a context, we further aggregate the path embeddings by the summation function to produce the *context embedding*, $\mathbf{c}_i = \sum_{j \in \mathcal{L}(l_k) \setminus \{i\}} \mathbf{p}_{i \rightarrow j}$. On the other hand, the assignments are simply encoded through an *one-hot* encoding. Therefore the final **operand embedding** $\mathbf{x}_i = (\mathbf{c}_i || \mathbf{v}_i)$, $\mathbf{x}_i \in \mathbb{R}^{d_c + d_v}$ is the concatenation of the **context embedding** ($\mathbf{c}_i \in \mathbb{R}^{d_c}$), and the corresponding one-hot **assignment encoding** ($\mathbf{v}_i \in \mathbb{R}^{d_v}$).

Computing weighted sum: We propose a novel module to compute attention weights using the *operand embeddings*. It has an (i) aggregation layer and an (ii) attention layer.

i) **Aggregation layer.** From the domain perspective, we design an aggregation step that allows for computing a *relative* importance score for each operand. This *importance* score reflects the *relative* influence of an operand to determine an output value, when compared to all the other operands in the same

statement l_k . We create an *updated operand embedding*, \mathbf{x}_i^* which captures the *relative importance* and produces a better representation than \mathbf{x}_i .

To do so, we augment a single attention head with a special *aggregation layer*. For each statement l_k , we aggregate all the operand embeddings using the sum function. Further, we aid the aggregation with a *skip-connection* weighted by a learnable parameter ϵ . The *updated operand embeddings* is as follows:

$$\mathbf{x}_i^* = MLP_{\theta_1} \left(\sum_{j \in \mathcal{L}(l_k)} \mathbf{x}_j + \epsilon \cdot \mathbf{x}_i \right), \mathbf{x}_i^* \in \mathbb{R}^{d_a}$$

ii) **Attention layer.** We use the *updated embeddings* to compute the attention weights. If a statement l_k has $N_i^{l_k}$ operands, $\mathbf{X}_{l_k}^* \in \mathbb{R}^{N_i^{l_k} \times d_a}$ is the matrix obtained from the stacking all the *updated operand embeddings*. The $\mathbf{X}_{l_k} \in \mathbb{R}^{N_i^{l_k} \times (d_c + d_v)}$ is the operand embedding matrix and $\mathbf{A} \in \mathbb{R}^{N_i^{l_k} \times d_a}$ is built by repeating the attention vector \mathbf{a} for $N_i^{l_k}$ times. Attention weights are computed as follows:

$$Attention(\mathbf{A}, \mathbf{X}_{l_k}^*, \mathbf{X}_{l_k}) = softmax(\mathbf{A} \mathbf{X}_{l_k}^{*T}) \mathbf{X}_{l_k}$$

Final prediction: We use the attention weights to compute a weighted summation of operand embeddings to generate the final embedding for a statement l_k . We use this embedding for the final prediction through MLP_{θ_2} . We train VeriBug end-to-end and it **learns execution semantics** from the simulation data. Attention weights for each prediction contain rich *execution* information which we use for **bug localization**.

Training Loss: We train our model with a cross-entropy loss using the ground-truth extracted from the simulation traces. To account for an unbalanced data set, we weight our loss with *inverse class frequencies* in the train set. We observe that training with this loss function barely updates the value of the attention head from its initialization value. To address this, we augment the previous loss function with a *regularization* term to update the model parameters more accurately. For a batch \mathcal{X}_B of training samples, the updated loss is as follows:

$$\mathcal{L}(\mathcal{X}_B) = \frac{\sum_{i=1}^N CE(y_i, \tilde{y}_i)}{\sum_{i=1}^N w_0 \mathbb{1}_{\tilde{y}_i=0} + w_1 \mathbb{1}_{\tilde{y}_i=1}} + \frac{\alpha}{N} \sum_{i=0}^N \frac{1}{\|\mathbf{X}_i^*\|}$$

where $y_i = y(l_i), \forall i \in \mathcal{X}_B$ is model prediction, \tilde{y}_i is ground-truth, $\mathbb{1}$ is the indicator function, α is a weighting factor for the regularization term, (w_0, w_1) are loss weights, \mathbf{X}_i^* are the *updated operand embeddings* for statement l_i , and $\|\cdot\|$ is a matrix norm. While the *first term is to train a predictor*, the *second term is dependent on our bug localization task*. Specifically, the second term helps to update the aggregation and projection layer parameters and accurately find the **importance** of each operand by computing attention scores.

D. Generating explanations of localization

The *Explainer* uses the learned execution semantics to produce the final heatmap \mathbb{H}_t . VeriBug enables **finer-grained localization** by mapping \mathbb{H}_t back to the Verilog code. We generate the heatmap using the attention weights produced by our DL model on multiple inference steps.

Attention maps: We refer the attention weights for a statement as its *explanation* of suspiciousness of being buggy. Intuitively, attention weights capture execution effect of a design statement on the target output. If the attention weights of a statement substantially differ in passing and failing traces, it indicates significantly different execution behavior of the statement, thereby raising suspicion. We aggregate the explanations of all the statements in the dynamic slice of \mathbf{t} and create an *attention map* which represents relative suspiciousness of different statements in the slice.

Aggregated maps and heatmap generation: A heatmap can be generated by comparing attention maps generated from *failure traces* (\mathcal{T}_f) and *correct traces* (\mathcal{T}_c). A trace is a *failure trace* if a bug is symptomatized at one of the outputs of \mathbf{D} , otherwise, it is considered a *correct trace*. We further aggregate all the attention maps within the two sets, producing two *aggregated maps* that summarize the design behavior in two different sets of traces. The aggregation is performed by computing a *statement-wise* average of the predicted attention weights. We denote these aggregation as \mathbb{F}_t and \mathbb{C}_t for failing and correct traces, respectively. To generate a heatmap \mathbb{H}_t , we make a *statement-wise* comparison of these two maps. Intuitively, if a design statement shows a significantly different execution behavior in the correct and failure traces, then the corresponding attention weights for that statement would be significantly different in \mathbb{F}_t and \mathbb{C}_t . **We highlight those design statement(s) as likely buggy candidates for debugging.**

Depending on the construction of the dynamic slices for \mathbf{t} , \mathbb{F}_t and \mathbb{C}_t may not contain information about the same set of statements. Thus, for a systematic comparison, we identify following three possible scenarios:

- **A statement l_k is present in \mathbb{C}_t but absent in \mathbb{F}_t .** We can infer that l_k is *not suspicious*, as \mathcal{T}_f do not record executions for l_k , thus it cannot cause a bug to symptomatize at \mathbf{t} .
- **A statement l_k is present in \mathbb{F}_t but absent in \mathbb{C}_t .** The execution of l_k affects the \mathbf{t} only in \mathcal{T}_f , causing a bug to symptomatize at \mathbf{t} . Thus, we mark l_k as *suspicious* and copy its attention weights from the \mathbb{F}_t to the final heatmap \mathbb{H}_t .
- **A statement is present in \mathbb{F}_t and \mathbb{C}_t .** This is a non-trivial case requiring further analysis. We identify this statement as *highly likely suspicious* if its attention weights **significantly differ** between \mathbb{F}_t and \mathbb{C}_t . To compute this difference, we use a *normalized* norm-1 distance. We apply min-max normalization on this distance, with $min = 0$ and $max = 2$, as a norm-1 distance between two sets of our attention weights always falls in this range. The computed difference is compared with a user-defined *suspicious threshold*; we set it to 0.10 for our analysis. When a statement is classified as *suspicious*, we move \mathbb{F}_t weights for l_k to the final \mathbb{H}_t .

Following this process, the final heatmap \mathbb{H}_t contains only attention weights of *candidate buggy statements*.

V. EXPERIMENTAL SETUP

Dataset generation: We train VeriBug on a *synthetic* data set to force variability in training data, necessary to achieve generalization. Our synthetic *Random Verilog Design Generator*

(RVGD) randomly generates Verilog designs using pre-defined template as follows. It has two distinct parts. In the first part, we have a *clocked always* block (C) that acts as a memory element to remember the current design state. The other *non-clocked always* block ($\mathcal{N}C$) computes the next state of the design based on the current state of the design and current inputs. It also assigns Boolean values to one or more design outputs. The $\mathcal{N}C$ contains multiple *if-else-if* blocks, each block computing using blocking assignments. RVGD randomly generates legal blocking assignments following Verilog’s grammar. RVGD ensures the presence of interdependencies among design variables to create data flows. RVGD also controls the maximum number of operands and Boolean operators in each design statement.

Training model: We used the *Adam* optimizer [5] for *mini-batch* stochastic gradient descent, with learning rate $lr = 10^{-3}$ and weight decay $wd = 10^{-5}$. We create batches by sampling statements and their associated input vectors from the training set. In the case of statement *inter-dependencies* requiring past predictions, ground truth results are used during training. At inference time, we obtain predictions following the correct statement order. This training strategy allows much faster training. We also set $d_a = 32$ as size for the attention vector, and $d_c = 16$ as the dimension of the context embedding vector. With this configuration, VeriBug takes a few minutes to train.

Bug injection: To validate the bug localization effectiveness we inject bugs of varying complexity on real-designs. Table I shows details for the realistic designs of our analysis. In this setup, *data-centric* bugs are introduced by automatically *mutating* the designs according to a pre-defined set of mutation rules. Specifically, we introduce *three* different types of bugs: (i) **Negation**, where the injected bug introduces a wrong “NOT” (\neg) in front of an operand or removes an existing one; (ii) **Variable misuse**, where a variable name is changed with another one, possibly syntactically similar. This replicates traditional human *copy-paste* errors; (iii) **Operation substitution**, where a Boolean operator is substituted with a wrong one, e.g., an “OR” (\vee) replaced with a “AND” (\wedge). To avoid undesirable masking behaviors, we inject one bug per mutated design. A bug is *observable* if the bug symptomatizes at design outputs.

Target predictor selection: Predictor performance could *theoretically* rely on α , the weighing factor of the *regularization* term introduced for the bug localization task (c.f., Training loss in Section IV-C). Hence, we evaluate predictor performance for different α values. We evaluate the predictors based on the quality of predicting the output value of a statement, on a test-set of *holdout* synthetic designs. We assume that the predictors with higher prediction accuracy are able to compute better statement representations and in general learn better *features* related to execution semantics. As we have an unbalanced test set, we also compute *precision* and *recall* obtained for both target bit values. We report these results in Table II. We observe that there is no substantial change in performances. However, $\alpha = 0.10$ produces slightly higher prediction accuracy, precision, and recall. Hence, we choose $\alpha = 0.10$ for our experiments.

TABLE I: **Details of modules in our localization test set.**

Module Name	Line of Codes	Short Description
wb_mux_2	65	<i>Wishbone 2-port Multiplexer</i>
usbf_pl	287	USB2.0 Protocol Layer
usbf_idma	627	USB2.0 Internal DMA Controller
ibex_controller	459	Ibex RISC-V Processor Controller

TABLE II: **Results on test-set obtained for different weighting α factors.** Pr = Precision, Re = Recall, Target = bit-level prediction class. We choose the predictor with $\alpha = 0.1$ as it exhibits the best execution semantics learning abilities, correctly predicting bit values of the outputs in almost all cases.

α	Acc. (%)	Pr/Re (Target 0)	Pr/Re (Target 1)
0.01	96.5	0.99/0.96	0.93/0.98
0.05	93.8	0.96/0.94	0.90/0.93
0.10	98.0	0.98/0.99	0.98/0.96
0.15	95.6	0.95/0.97	0.96/0.92
0.20	96.7	0.97/0.98	0.96/0.95
0.25	97.7	0.97/0.99	0.99/0.95

VI. EXPERIMENTAL RESULTS

A. Bug Coverage Results on Open-Source Designs

In this section, we evaluate the effectiveness of VeriBug for bug localization using realistic designs. We show our localization results in Table III. We compute a bug coverage metric for each design-target pair as the ratio between the number of localized bugs and the total number of observable bugs. We consider a bug as localized when the highest suspiciousness score in the heatmap \mathbb{H}_t is assigned to the statement containing the root cause. Thus, we compute a top-1 bug coverage metric. Note that a localization error (*i.e.*, coverage reduction) could be due to either the suspiciousness score is not the highest in heatmap or a statement’s exclusion from the heatmap due to suspiciousness score lower than the user-defined threshold. We consider the highest suspiciousness scores after running the same VeriBug instance over multiple simulation runs.

We observe that VeriBug is effective in localizing different bug types in data-flow, especially for the *ibex_controller* (97.6% of top-1 bug coverage) and the *wb_mux_2* (87.5% of top-1 bug coverage) designs. The two USB modules, *usbf_idma* and the *usbf_pl* have lower bug coverage with 70.8% and 63.6% coverage respectively. For the former, this is due to the difficulty in finding the injected bug on the target output as we report in Table III. Considering all designs and injected bugs, we obtain an overall top-1 bug localization coverage of 82.5%. This experiment shows that VeriBug is a promising approach for precise bug localization of data-centric bugs. Note, we train VeriBug on synthetic designs, yet it localizes well in realistic designs. This empirical evidence shows that the learned knowledge is transferable making our approach as a promising one for broader adoption.

B. Exact Root-Cause Localization via VeriBug Heatmaps

VeriBug allows for further localization via mapping importance scores stored in heatmap \mathbb{H}_t back to the RTL code. In this experiment we evaluate how these importance scores help in bug localization. We show some examples of VeriBug generated heatmaps on realistic designs in Figure 4. Together with

TABLE III: **Bug coverage for bug-localization on realistic designs.** For each injected bug-type, we show number of design versions. We compute top-1 coverage by considering observable bugs on the target output and the number of localized bugs.

Design Name	Target	Injected Bugs				↑ top-1 Coverage (%)
		<i>Negation</i>	<i>Operation</i>	<i>Misuse</i>	Total (Observable)	
wb_mux_2	wbs0_we_o	2	2	4	8 (8)	87.5% (7/8)
wb_mux_2	wbs0_stb_o	2	2	4	8 (8)	87.5% (7/8)
wb_mux_2	-	4	4	8	16 (16)	87.5% (14/16)
usbf_pl	match_o	5	8	9	22 (10)	60.0% (6/10)
usbf_pl	frame_no_we	3	4	9	16 (12)	66.6% (8/12)
usbf_pl	-	8	12	18	38 (22)	63.6% (14/22)
usbf_idma	mreq	3	4	6	13 (12)	50.0% (6/12)
usbf_idma	adr_incw	2	2	8	12 (12)	91.6% (11/12)
usbf_idma	-	5	6	14	25 (24)	70.8% (17/24)
ibex_controller	stall	4	6	12	22 (22)	95.4% (21/22)
ibex_controller	instr_valid_clear_o	3	4	12	19 (19)	100% (19/19)
ibex_controller	-	7	10	24	41 (41)	97.6% (40/41)
Overall	-	24	32	64	120 (103)	82.5% (85/103)

Module Name	$\mathbb{C}_t(l_{bug})$	$\mathbb{H}_t/\mathbb{F}_t(l_{bug})$
WB MUX2	assign wbs0_dat_o = wbm_dat i; /* mutant no: 7 :: assign wbs0_we_o = wbm_we_i & wbs0_sel;*/ assign wbs0_we_o = wbm_we_i & ~wbs0_sel; assign wbs0_sel_o = wbm_sel i;	assign wbs0_dat_o = wbm_dat i; /* mutant no: 7 :: assign wbs0_we_o = wbm_we_i & wbs0_sel;*/ assign wbs0_we_o = wbm_we_i & ~wbs0_sel ; assign wbs0_sel_o = wbm_sel i;
USB PL	// Frame Number (from SOF token) /* mutant no: 2 :: assign frame_no_we = token_valid & !crc5_err & pid_SOF;*/ assign frame_no_we = token_valid & !crc5_err pid_SOF ;	// Frame Number (from SOF token) /* mutant no: 2 :: assign frame_no_we = token_valid & !crc5_err & pid_SOF;*/ assign frame_no_we = token_valid & !crc5_err pid_SOF ;
USB IDMA	// Memory Request /* mutant no: 1 :: assign mreq = (mreq_d & !mack_r) word_done_r;*/ assign mreq = (mreq_d ^ !mack_r) word_done_r ;	// Memory Request /* mutant no: 1 :: assign mreq = (mreq_d & !mack_r) word_done_r;*/ assign mreq = (mreq_d ^ !mack_r) word_done_r ;
IBex RISC-V Controller	assign debug_mode_o = debug_mode q; /* mutant no: 8 :: assign stall = ((stall_lsu_i stall_multdiv_i) stall_jump_i) stall_branch_i;*/ assign stall = ((stall_lsu_i stall_multdiv_i) stall_jump_i) stall_branch_i ; assign id_in_ready_o = (~stall & ~halt_i); assign instr_valid_clear_o = (~stall halt_i) flush_id;	assign debug_mode_o = debug_mode q; /* mutant no: 8 :: assign stall = ((stall_lsu_i stall_multdiv_i) stall_jump_i) stall_branch_i;*/ assign stall = ((stall_lsu_i stall_multdiv_i) stall_jump_i) stall_branch_i ; assign id_in_ready_o = (~stall & ~halt_i); assign instr_valid_clear_o = (~stall halt_i) flush_id;

Fig. 4: **VeriBug qualitative results on realistic designs: examples of VeriBug generated heatmaps.** For comparison, we also report the operand importance scores (blue, deeper is more important) in \mathbb{C}_t , against which important scores (red, deeper is more important) in \mathbb{F}_t are compared. The rightmost column reports the *suspiciousness* score for the statement l_{bug} (i.e., the statement with the root cause). Note that $\mathbb{H}_t(l_{bug}) = \mathbb{F}_t(l_{bug})$ when *suspiciousness* score for l_{bug} is higher than threshold.

heatmaps \mathbb{H}_t , we also provide a visualization of scores stored in \mathbb{C}_t . To offer better visualization, we discretize the range $[0, 1]$ into bins, assigning a different color intensity to each bin, in the scale of reds for \mathbb{H}_t and blues for \mathbb{C}_t . We also report the corresponding *suspiciousness* score $d(\mathbb{F}_t(l_{bug}), \mathbb{C}_t(l_{bug}))$.

Heatmaps visualized in Figure 4 show how, in failure traces \mathcal{T}_f , **a higher importance score is assigned to operands that are source of bugs or are directly involved in an buggy operation.** We also show how **different importance scores are assigned to the same operands for correct traces \mathcal{T}_c , where the bug is instead masked.** Results obtained for the *usbf_idma* and *ibex_controller* modules also justify our choice of selecting 0.1 as our default threshold for the suspiciousness score, as a score higher than this corresponds to a visual difference in the two maps. This experiment shows that VeriBug is able to learn low-level execution semantics details. It can effectively use such learned knowledge to localize the bug and provide necessary explanations at source-code level for debugging.

VII. CONCLUSION

We present VeriBug, which relies on Attention and LSTM-based DL model to learn RTL execution semantics. VeriBug uses a novel approach to repurpose the learned semantic knowledge for bug localization. VeriBug is unique as compared to the other state-of-the-art techniques as it localizes the bug and generates explanation automatically to make its decision

accessible to a debugging engineer. We also show VeriBug is particularly effective for data-flow bug localization and its learned knowledge is transferable. Albeit very preliminary, our approach shows promising results and it is compatible with current verification flows without any additional artifacts.

REFERENCES

- [1] D. Bahdanau, K. Cho, and Y. Bengio. Neural Machine Translation by Jointly Learning to Align and Translate. *Int'l Conf. on Learning Representations (ICLR)*, 2016.
- [2] A. R. Bradley. Understanding IC3. *Int'l Conf. on Theory and Applications of Satisfiability Testing (SAT)*, 2012.
- [3] R. Bryant. Graph-Based Algorithms for Boolean Function Manipulation. *IEEE Trans. on Computers (TC)*, 1986.
- [4] E. Clarke, A. Biere, R. Raimi, and Y. Zhu. Bounded Model Checking Using Satisfiability Solving. *Formal Methods in System Design (FMSD)*, 2001.
- [5] D. P. Kingma and J. Ba. Adam: A Method for Stochastic Optimization. *Int'l Conf. on Learning Representations (ICLR)*, 2017.
- [6] Y. Li, S. Wang, T. N. Nguyen, and S. Van Nguyen. Improving Bug Detection via Context-Based Code Representation Learning and Attention-Based Neural Networks. *Proc. of the ACM on Programming Languages (PACMPL)*, 2019.
- [7] K. L. McMillan. Interpolation and SAT-Based Model Checking. *Int'l Conference on Computer Aided Verification (CAV)*, 2003.
- [8] D. Pal, S. Offenberger, and S. Vasudevan. Assertion Ranking Using RTL Source Code Analysis. *IEEE Trans. on Computer-Aided Design of Integrated Circuits and Systems (ICAD)*, 2020.
- [9] D. Pal and S. Vasudevan. Symptomatic Bug Localization for Functional Debug of Hardware Designs. *Int'l Conf. on VLSI Design Embedded Systems (VLSID)*, 2016.

- [10] D. E. Rumelhart, G. E. Hinton, R. J. Williams, et al. Learning Internal Representations by Error Propagation. *Parallel Distributed Processing: Explorations in the Microstructure of Cognition: Foundations*, 1985.
- [11] S. Wang, D. Chollak, D. Movshovitz-Attias, and L. Tan. Bugram: Bug detection with n-gram language models. *Int'l Conf. on Automated Software Engineering (ASE)*, 2016.